Cohen and D. A. D. Parry, *Proteins* **7**, 1 (1990).
17. DNA encoding the Tar c-fragment (residues 257 to 553) (Fig. 2B) (*32, 33*) was ligated into the T7 expression vector pAED4 [D. S. Doering, thesis, Massachusetts Institute of Technology (1992)] according to standard molecular cloning protocols [J. Sambrook, E. F. Fritsch, T. Maniatis, *Molecular Cloning: A Laboratory Manual* (Cold Spring Harbor Laboratory, Cold Spring Harbor, NY, ed. 2, 1989)]. The EEEE and QQQQ variants were obtained by in vitro mutagenesis (Amersham kit RPN 1523) of the c-fragment construct. An expression vector (p4LZ) encoding residues 2 to 33 of the GCN4 dimerization domain has been described [K. J. Lumb, C. M. Carr, P. S. Kim, *Biochemistry* **33**, 7361 (1994)]; the coding sequence was modified here to include two additional amino acids (Lys-Val) after the initiating methionine to yield plasmid pGCN4-pR (Fig. 2C). The encoded GCN4-pR peptide is fully folded as judged by its circular dichroism spectrum. The GCN4-Tar chimeras were obtained by joining the two constructs with short synthetic linkers encoding the sequences shown in Fig. 2C. Proteins were expressed in *E. coli* strain RP3098, from which the *che* genes have been deleted [R. S. Smith and J. S. Parkinson, *Proc. Natl. Acad. Sci. U.S.A.* **77**, 5370 (1980)]. The GCN4 fusion proteins were purified essentially as described for the c-fragment (*34*). Concentrations of dialyzed proteins were determined from their absorbance spectra in 6 M guanidine hydrochloride [H. Edelhoch, *Biochemistry* **6**, 1948 (1967)].
18. C. M. Carr, thesis, Massachusetts Institute of Technology (1995); J. A. Zitzewitz, O. Bilsel, J. Luo, B. E. Jones, C. R. Matthews, *Biochemistry* **34**, 12812 (1995).
19. The genes of the bacterial chemotaxis receptors encode a mixture of glutamic acid (E) and glutamine (Q) at the major cytoplasmic methylation sites. For Tar, the residues are Q295, E302, Q309, and E491, or QEQE, in the newly synthesized receptors (*32*).
20. K. A. Borkovich, N. Kaplan, J. F. Hess, M. I. Simon, *Proc. Natl. Acad. Sci. U.S.A.* **86**, 1208 (1989).
21. K. A. Borkovich and M. I. Simon, *Methods Enzymol.* **200**, 205 (1991); J. F. Hess, R. B. Bourret, M. I. Simon, *ibid.*, p. 188.
22. Chemotaxis proteins CheW, CheA, and CheY were produced from overexpression plasmids (*35*) and purified according to standard protocols (*21, 36*). Concentrations of purified proteins were determined as described (*17*). Each reaction mixture (10 μl final volume) contained the appropriate purified receptor fragment (20 μM), 2 μM CheW, 0.1 μM CheA, and 15 μM CheY in 50 mM tris-HCl (pH 7.5), 50 mM KCl, 5 mM $MgCl_2$, and 10% (w/v) glycerol. Protein mixtures were incubated for 6 hours at room temperature before initiation of the reaction by addition of 1 μl of 1 mM [γ-^{33}P]adenosine triphosphate (~10^4 cpm/pmol) (DuPont Biotechnology Systems). Reactions were quenched after 10 s by addition of 5 μl of 2× SDS loading buffer containing 25 mM EDTA (*21*), and the entire volume was applied (without heating) to denaturing 10% polyacrylamide–tricine gels (0.075 by 7 by 10 cm) [H. Schagger and G. von Jagow, *Anal. Biochem.* **166**, 368 (1987)]. After electrophoresis at 85 V, gels were stained with Coomassie blue, dried, and subjected to quantitative autoradiography (*21*) (FUJIX BAS 2000).
23. Kinase stimulation by tumble-mutant fragments of the *E. coli* serine receptor (Tsr) [P. Ames and J. S. Parkinson, *J. Bacteriol.* **176**, 6340 (1994)] requires a much higher fragment concentration than did kinase stimulation by soluble GCN4-Tar dimers. The protein concentrations used here (*22*) were identical to those used in assays of intact Tar in membrane vesicles (*11*) but included an approximately fivefold higher concentration of receptor; the extents of CheA stimulation were comparable.
24. Circular dichroism studies confirmed that all fusion proteins were folded and differed only slightly in secondary structure content at low temperatures. {The QQQQ variants [θ_{222} (mean residue ellipticity) = −23,000 degree cm^2 dmol^{-1} at 0°C] were somewhat more helical than the QEQE or EEEE variants (θ_{222} = −18,000 degree cm^2 dmol^{-1} at 0°C).} Thermal denaturation studies revealed a distinct transition midpoint for each interdomain linkage (with apparent midpoints of 52°, 57°, and 64°C, for the QEQE variants of **8**, **5**, and **9**, respectively, at 1.3 μM receptor), consistent with the idea that the receptor conformation has been strained by shifting the dimer interface. These midpoints were unaffected by methylation site mutations.
25. Samples (5 μM) were analyzed at 9000, 11,000, and 14,000 rpm in a Beckman XL-A centrifuge. Centrifuge temperature was 10°C for samples lacking glycerol and 20°C for those containing glycerol; sample buffer was 5 mM tris-HCl (pH 7.5), 50 mM KCl, and 5 mM $MgCl_2$. Data sets (six to eight per protein) were fitted simultaneously to a single-species model with the program NONLIN [M. L. Johnson, J. J. Correia, D. A. Yphantis, H. R. Halvorson, *Biophys. J.* **36**, 575 (1981)] to yield an apparent σ value. Expected monomer σ values were calculated with partial specific volumes based on amino acid composition as described [T. M. Laue, B. D. Shah, T. M. Ridgeway, S. L. Pelletier, in *Analytical Ultracentrifugation in Biochemistry and Polymer Science*, S. E. Harding, A. J. Rowe, J. C. Horton, Eds. (Royal Society of Chemistry, Cambridge, 1992), pp. 90–125].
26. D. L. Milligan and D. E. Koshland Jr., *Science* **254**, 1651 (1991).
27. Reviewed in C.-H. Heldin, *Cell* **80**, 213 (1995).
28. A. M. de Vos, M. Ultsch, A. A. Kossiakoff, *Science* **255**, 306 (1992); W. Somers, M. Ultsch, A. M. de Vos, A. A. Kossiakoff, *Nature* **372**, 478 (1994).
29. D. W. Banner *et al.*, *Cell* **73**, 431 (1993).
30. S. R. Hubbard, L. Wei, L. Ellis W. A. Hendrickson, *Nature* **372**, 746 (1994).
31. J. R. Maddock and L. Shapiro, *Science* **259**, 1717 (1993).
32. A. Krikos, N. Mutoh, A. Boyd, M. I. Simon, *Cell* **33**, 615 (1983).
33. K. Oosawa, N. Mutoh, M. I. Simon, *J. Bacteriol.* **170**, 2521 (1988).
34. N. Kaplan and M. I. Simon, *ibid.*, p. 5134; D. G. Long and R. M. Weis, *Biochemistry* **31**, 9904 (1992).
35. J. A. Gegner, D. R. Graham, A. F. Roth, F. W. Dahlquist, *Cell* **70**, 975 (1992).
36. J. A. Gegner and F. W. Dahlquist, *Proc. Natl. Acad. Sci. U.S.A.* **88**, 750 (1991).
37. W. T. Pu and K. Struhl, *ibid.*, p. 6901.
38. We thank F. W. Dahlquist for providing expression plasmids for CheA, CheW, and CheY; J. S. Parkinson for providing *E. coli* chemotaxis deletion strains; and K. M. Shokat and J. K. Judice for helpful comments on the manuscript. A.G.C. was supported by a National Science Foundation postdoctoral fellowship (CHE-9102242) and a Public Health Service training grant (T32 AI07348-07). This research was supported by the Howard Hughes Medical Institute.

2 August 1995; accepted 17 November 1995

Heparin Structure and Interactions with Basic Fibroblast Growth Factor

S. Faham, R. E. Hileman, J. R. Fromm, R. J. Linhardt,* D. C. Rees*

Crystal structures of heparin-derived tetra- and hexasaccharides complexed with basic fibroblast growth factor (bFGF) were determined at resolutions of 1.9 and 2.2 angstroms, respectively. The heparin structure may be approximated as a helical polymer with a disaccharide rotation of 174° and a translation of 8.6 angstroms along the helix axis. Both molecules bound similarly to a region of the bFGF surface containing residues asparagine-28, arginine-121, lysine-126, and glutamine-135; the hexasaccharide also interacted with an additional binding site formed by lysine-27, asparagine-102, and lysine-136. No significant conformational change in bFGF occurred upon heparin oligosaccharide binding, which suggests that heparin primarily serves to juxtapose components of the FGF signal transduction pathway.

Despite the importance of heparin and related glycosaminoglycans as components of the extracellular matrix, as participants in signal transduction pathways, and as therapeutic agents, atomic resolution structures are not available for heparin-based species larger than monosaccharides [reviewed in (*1*)]. This absence of precise structural information reflects difficulties in obtaining homogenous samples of heparin-derived molecules. The heparin polymer consists of a basic disaccharide repeat unit comprised of L-iduronic acid (Idu) and D-glucosamine (GlcN) joined by α(1→4) linkages (Fig. 1A). A typical heparin disaccharide contains a total of three sulfate groups: one attached to the 2-hydroxyl group of Idu and two linked to the 2-amino and 6-hydroxyl groups of GlcN. The related glycosaminoglycan heparan sulfate has a similar structure containing D-glucuronic acid, L-Idu, and D-GlcN but is less extensively sulfated. Successive disaccharides within heparin are related by a twofold screw operation, generated by a rotation angle of ~180° coupled to a translation of ~8.0 to 8.7 Å along the helix axis (*2*). The structure of heparin may be approximated by a ribbon with sulfate and carboxyl groups on the edges and hydroxyl and sugar ring oxygen atoms positioned on the surfaces between these negatively charged groups. Although the average structure of heparin is defined, local structural alterations exist within the heparin polymer that are a result of heterogeneity in the sequence, conforma-

S. Faham and D. C. Rees, Division of Chemistry and Chemical Engineering 147-75CH, California Institute of Technology, Pasadena, CA 91125, USA.
R. E. Hileman, J. R. Fromm, R. J. Linhardt, Division of Medicinal and Natural Products Chemistry, College of Pharmacy, University of Iowa, Iowa City, IA 52242, USA.

*To whom correspondence should be addressed. E-mail: rees@citray.caltech.edu and linhardt@blue.weeg.uiowa.edu

tion, and pattern of sulfation, all of which may be important for the polymer's interactions with other biomolecules.

The participation of proteoglycans related to heparin in signal transduction pathways is exemplified by their involvement in the initial binding events between members of the fibroblast growth factor (FGF) family and their associated tyrosine kinase receptors [reviewed in (3)]. Heparin-like molecules may enhance the activity of FGFs, either through binding-induced changes in the structure and stability of FGF or by direct participation in FGF-receptor interactions, possibly by binding to both components or by binding multiple FGF molecules to facilitate receptor dimerization (*4–8*). Aside from their role in mediating FGF-receptor interactions, heparan sulfate proteoglycans in the extracellular matrix may also function to help sequester and localize FGFs in the vicinity of the cell surface. These functional properties reflect sequence-specific structural features of heparin and other sulfated proteoglycans that permit productive binding interactions with FGFs.

To establish a framework for probing the structures of heparin-related molecules and their interactions with proteins, we initiated a crystallographic analysis of the heparin–basic FGF system. Because heparin itself is too heterogeneous to be compatible with crystallization, homogeneous tetra- and hexasaccharide fragments of heparin (Fig. 1B) were prepared by heparinase digestion, purified to homogeneity, and structurally characterized (*9*). These fragments of heparin bind specifically to FGFs with dissociation constants that are similar to those for heparin reported by Mach *et al.* (*10*).

After co-crystallizations of bFGF with both the tetra- and hexasaccharide heparin fragments (*11*), the structures of these complexes were solved and refined at resolutions of 1.9 and 2.2 Å, respectively (*12*) (Fig. 2). The two heparin fragments have essentially the same structure and make the same contacts with bFGF when possible (Fig. 3). The helical parameters of the heparin helix were estimated from the hexamer structure (*13*); the average observed helical parameters of a 174° rotation and an 8.6 Å translation per disaccharide are in good agreement with the x-ray fiber diffraction values of 180° and 8.0 to 8.7 Å, respectively, for the heparin polymer (*2*). The observed torsion angles of the heparin hexamer fall within the calculated allowed region for the heparin polymer and are close to those previously derived from nuclear magnetic resonance data (*14*). A stereochemically significant aspect of the heparin structure is the conformation of the six-membered hexopyr-

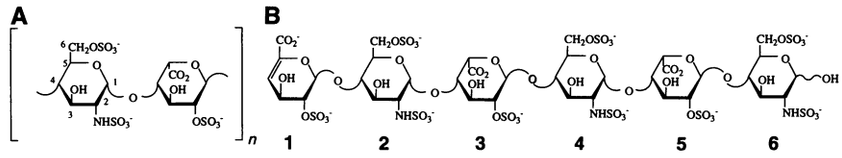

Fig. 1. (**A**) Chemical structure of the repeating disaccharide of heparin. (**B**) Structure of the heparin hexasaccharide fragment used for the crystallographic studies. The numbering system used here to identify the different sugar rings is indicated, with the nonreducing and reducing rings assigned numbers 1 and 6, respectively. The analogous numbering system is used for the tetrasaccharide, except that the reducing sugar is assigned ring number 4.

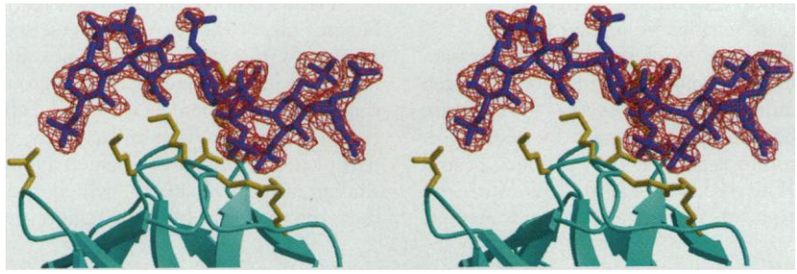

Fig. 2. $F_o - F_c$ difference electron density map of the bFGF-hexasaccharide complex calculated at 2.2 Å resolution, with the hexasaccharide omitted from the structure factor calculation. The map (red) is contoured at 1.8 times the overall root-mean-square value of the map, with the refined structure of the hexasaccharide (blue) superimposed. The polypeptide chain of bFGF and the side chains of residues that interact with the hexasaccharide are represented in cyan and yellow, respectively.

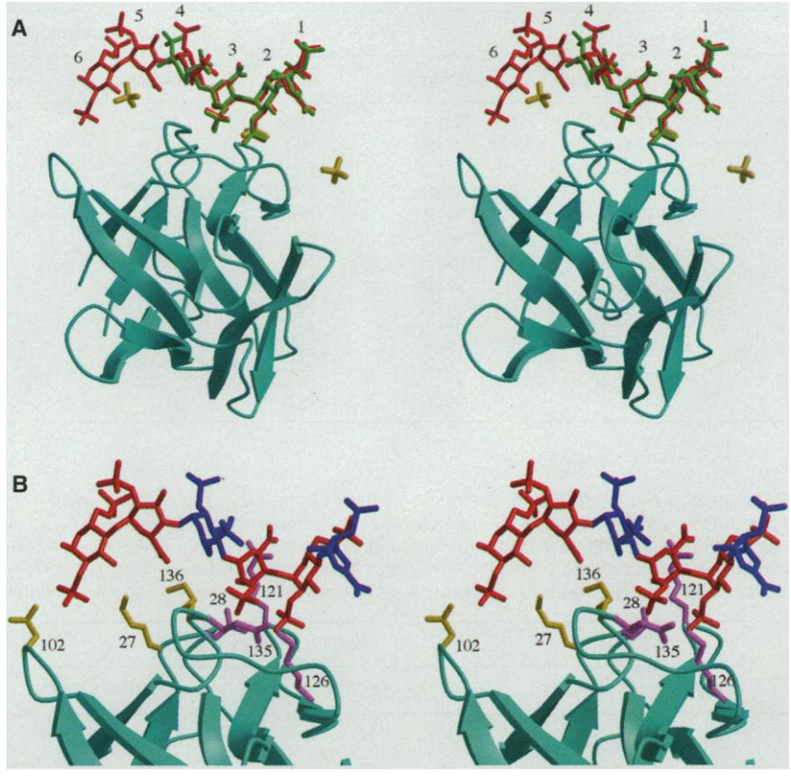

Fig. 3. (**A**) Stereodiagram of a superposition of the tetrasaccharide (green) and hexasaccharide (red) heparin fragments binding to bFGF. The sulfate ions located in a crystallographic analysis of unliganded bFGF (*17*) are represented by yellow. (**B**) Stereodiagram illustrating specific interactions between bFGF and the hexasaccharide fragment. The higher affinity binding site is colored magenta, whereas the lower affinity binding site is colored yellow. Sugar rings 1 and 3, which do not contact this region of bFGF, are blue. The side chains and residue numbers of amino acids in bFGF that interact with the hexasaccharide are indicated. Structural figures for this paper were prepared with the program MOLSCRIPT (*28*).

anose ring of the Idu residues, which can exist in a chair form designated $^1C_4$ or in a skew boat conformation termed $^2S_0$ (*15*). The hexasaccharide fragment of heparin used here contains two Idu rings: Idu-3 of the hexamer was observed to be in the $^1C_4$ chair conformation, whereas Idu-5 adopted the $^2S_0$ skew boat conformation. Consequently, multiple conformations of Idu can be adopted in the binding of heparin to FGF, and the conformational flexibility of this residue may play a role in the recognition and binding properties of heparin to its various biological ligands.

The structures of the heparin tetrasaccharide and hexasaccharide cocrystallized with human bFGF directly demonstrate that the primary binding site for heparin on this protein is generated by residues 27 and 28, 101 to 103, and 120 to 137. With the exception of the region around Asn[102], these assignments are in overall agreement with those of previously identified bFGF residues associated with heparin binding (*16–22*). The surface area (*23*) lost by bFGF residues upon binding of the tetrasaccharide and the hexasaccharide to bFGF may be calculated to be ~180 and ~290 Å^2, respectively. The larger contact region between bFGF and the hexasaccharide, relative to that of the tetrasaccharide, is consistent with the higher binding affinity of bFGF for the hexasaccharide as measured by microtitration calorimetry (*9*). Many, but not all, of the specific interactions between bFGF and the heparin hexamer are mediated by negatively charged groups on the heparin fragment (Fig. 3 and Table 1). For the sequences used in this study, rings 1 to 4 of the two heparin fragments bind in a similar fashion to bFGF, which indicates that the heparin binding region may be further separated into higher and lower affinity regions. The higher affinity site is defined as the region of the bFGF surface common to the binding of rings 2 and 3 of both fragments, whereas the lower affinity site is occupied by rings 5 and 6 only in the complex of the longer hexasaccharide with bFGF. The higher affinity binding site interacts with heparin through the side chains of residues Asn[28], Arg[121], Lys[126], and Gln[135], whereas the lower affinity site uses the side chains of residues Lys[27], Asn[102], and Lys[136]. The four residues that form the higher affinity region correspond exactly to the four residues identified by Thompson *et al.* (*16*) as having the greatest impact on the binding of bFGF to heparin.

Although other anionic compounds have been crystallographically observed to bind to the same general region of the FGF surface as these heparin fragments (*19–22*), because of their distinct chemical structures the specific interactions with FGF are generally different. One exception is provided by the 2-*N*-sulfate of GlcN-2 of the heparin fragments, which corresponds to a sulfate group of sucrose octasulfate (*21*) and a bound sulfate from crystallization of the unliganded protein (*17*) (Fig. 3A). Sulfate groups are not required for binding to this general region, however, because Ornitz *et al.* (*22*) found that a nonsulfated trisaccharide can bind to the higher affinity region of bFGF by using only carboxyl and hydroxyl group interactions with protein residues.

The conservation of residues forming the heparin binding region provides important indications concerning the extent to which other members of the FGF family can use binding interactions exhibited in these complexes of bFGF with heparin fragments. The FGF family currently consists of nine members, including bFGF, acidic FGF, HST, and KGF, with sequence identities varying from 30 to 55% (*24*). From a sequence alignment of this family,

Table 1. Polar (ion pair and hydrogen bond) contacts between bFGF residues and tetrasaccharide and hexasaccharide fragments of heparin. Interactions between atoms separated by less than 3.6 Å are indicated. The higher affinity region is defined by contacts involving GlcN-2 or Idu-3, whereas the lower affinity region involves contacts to Idu-5 or GlcN-6. Modeling studies suggest that the hexasaccharide fragment would form most of the contacts that a longer, linear heparin helix would make with a bFGF monomer. Lattice contacts involving polar interactions between the hexasaccharide and crystallographically related bFGF molecules were observed between atoms in ring 1 and R108 and N72; ring 2 and K47 and S48; and ring 6 and R34, H36, and E46 (*29*).

Heparin		bFGF		Closest distance (Å)	
Residue	Atom (or group)	Residue	Atom	Tetramer	Hexamer
GlcN-2	2-*N*-SO_3^-	N28	Nδ2	3.3	3.2
GlcN-2	2-*N*-SO_3^-	R121	NH	3.1	3.1
GlcN-2	2-*N*-SO_3^-	K126	Nζ	3.0	2.9
Idu-3	3-OH	N28	Oδ1	2.8	2.6
Idu-3	6-CO_2^-	R121	Nη1	3.2	3.1
Idu-3	2-*O*-SO_3^-	K126	Nζ	2.8	3.0
Idu-3	2-*O*-SO_3^-	Q135	Nε2	3.5	3.4
Idu-3	2-*O*-SO_3^-	K136	NH	3.0	3.1
Idu-3	2-*O*-SO_3^-	A137	NH	2.9	3.0
Idu-5	6-CO_2^-	K136	Nζ		3.3
GlcN-6	2-*N*-SO_3^-	K27	Nζ		3.6
GlcN-6	2-*N*-SO_3^-	N102	Nδ2		2.5
GlcN-6	3-OH	K27	Nζ		2.8

Table 2. Sequence alignment (*29*) of members of the FGF family in the heparin binding region. The Wisconsin Sequence Analysis Package, version 8, was used to generate the alignment (*30*). Heparin residues contacting side chain atoms of the indicated residues are listed. "High" affinity refers to contacts involving GlcN-2 or Idu-3, whereas "low" affinity refers to contacts involving Idu-5 or GlcN-6. The accession numbers for the bFGF, aFGF, INT2, HST, FGF5, FGF6, KGF, AIGF, and FGF9 sequences are A26642, A24820, S04742, Tvhuhs, Tvhuf5, S04204, A36301, A46245, and A48137, respectively, of the Protein Identification Resource protein sequence database.

Residue number	Residue of family member									Heparin contact	Affinity
	bFGF	aFGF	INT2	HST	FGF5	FGF6	KGF	AIGF	FGF9		
27	K	S	A	N	R	N	R	R	R	GlcN–2-*N*-SO_3^- GlcN3-OH	Low
28	N	N	T	V	V	V	T	T	T	GlcN–2-*N*-SO_3^- Idu3-OH	High
102	N	N	L	N	N	N	N	N	N	GlcN–2-*N*-SO_3^-	Low
121	R	K	G	K	K	K	Q	R	K	Idu3-OH	High
126	K	K	R	K	K	K	V	R	R	GlcN–2-*N*-SO_3^- Idu2–*O*-SO_3^-	High
135	Q	Q	Q	M	H	M	Q	Q	Q	Idu2–*O*-SO_3^-	High
136	K	K	K	K	I	T	K	R	K	Idu6-CO_2^-	Low

the conservation of residues with side chains that interact with heparin may be evaluated (Table 2). No residue in the heparin binding region is completely conserved throughout the FGF family; furthermore, even the charge of the residue side chain fails to be strictly maintained. As a result of these sequence variations, it is likely that different members of the FGF family use different contacts for the binding to heparin, as suggested by heparin desulfation experiments (8). For example, although bFGF makes a specific contact to the 2-O-sulfate group of Idu through the side chain of Gln^{135}, the substitution of this residue by Met in HST should interfere with this interaction, which is consistent with the observation that HST can bind heparin in the absence of 2-O-sulfate groups (8). Perhaps the most dramatic substitutions involve Asn^{28} and Lys^{126}, which are changed to Thr and Val, respectively, in KGF. These substitutions would be expected to block or alter the contact of these side chains with the GlcN 2-*N*-sulfate group in the high-affinity site. This alteration in the interaction between heparin and KGF relative to that of bFGF may contribute to the differential effects of heparan sulfates on KGF relative to their effects on acidic FGF (25).

The binding of these heparin fragments to bFGF is not associated with any significant conformational change in the polypeptide backbone; the root-mean-square deviation based on the Cα positions between the heparin hexamer–bFGF complex and the unbound bFGF is 0.34 Å. Similar observations have been reported for the binding of sucrose octasulfate (21) and nonsulfated trisaccharides to FGFs (22). Consequently, it appears unlikely that a heparin-induced conformational change in bFGF mediates initiation of the signal transduction pathway. Our results instead support heparin either binding multiple FGF molecules to promote receptor dimerization or facilitating formation of an FGF-receptor complex by binding both components (5–8). The possibility that protein-protein associations involved in signal transduction pathways may be regulated by binding interactions to specific molecules such as heparin is not unique to the FGF system, but rather reflects a mechanism of general biological relevance (26).

The heparin polymer contains about eight sugar residues in 34 Å along the helix axis, which is approximately the width of an FGF molecule. Consequently, FGFs could bind to one side of a heparin polymer with a density of one FGF molecule per eight sugar residues, as reported for bFGF (27). As observed in this crystal structure, however, not all of the heparin surface is buried in the interaction with FGF, so that binding sites along the heparin molecule would be available for interaction with additional ligands, such as other FGF molecules or the FGF receptor. These molecules could interact with heparin groups that are otherwise not used in FGF binding, such as the 6-O-sulfate groups, or they could bind to sites on heparin not occupied by FGF and interact with the same groups. With the sequence variability exhibited by both heparin and different members of the FGF family, a diverse set of binding interactions between FGFs and heparin-like molecules occurs, and these are reflected in the differing responses and requirements exhibited by the FGF family for these sulfated polysaccharides. In particular, variation in the carbohydrate sequence or sulfation pattern might be used to specify the presence or absence of binding sites in heparin for FGF and other molecules, thereby permitting assembly of the appropriate complex of molecules for the initiation of signal transduction.

REFERENCES AND NOTES

1. D. A. Lane and U. Lindahl, Eds., *Heparin* (CRC Press, Boca Raton, FL, 1989); L. Kjellen and U. Lindahl, *Annu. Rev. Biochem.* **60**, 443 (1991).
2. I. Nieduszynski, in *Heparin*, D. A. Lane and U. Lindahl, Eds. (CRC Press, Boca Raton, FL, 1989), pp. 51–63.
3. D. Gospodarowicz, N. Ferrara, L. Schweigerer, G. Neufeld, *Endocr. Rev.* **8**, 95 (1987); W. H. Burgess and T. Maciag, *Annu. Rev. Biochem.* **58**, 575 (1989); D. Benharroch and D. Birnbaum, *Isr. J. Med. Sci.* **26**, 212 (1990); C. Basilico and D. Moscatelli, *Adv. Cancer Res.* **59**, 115 (1992); J. Folkman and Y. Shing, *J. Biol. Chem.* **267**, 10931 (1992).
4. I. J. Mason, *Cell* **78**, 547 (1994).
5. D. M. Ornitz *et al.*, *Mol. Cell. Biol.* **12**, 240 (1992).
6. T. Spivak-Kroizman *et al.*, *Cell* **79**, 1015 (1994).
7. M. Kan *et al.*, *Science* **259**, 1918 (1993).
8. S. Guimond, M. Maccarana, B. B. Olwin, U. Lindahl, A. C. Rapraeger, *J. Biol. Chem.* **268**, 23906 (1993).
9. Tetrasaccharide and hexasaccharide fragments of porcine mucosal heparin were prepared by partial digestion with heparin lyase I, followed by preparative strong anion exchange high-performance liquid chromatography [A. Pervin, C. Gallo, K. A. Jandik, X.-J. Han, R. J. Linhardt, *Glycobiology* **5**, 83 (1995)]. As a product of this procedure, the heparin fragments contain an unsaturated uronic acid group at the nonreducing end and a mixture of α and β anomers at the reducing end of the oligosaccharide. Consequently, the tetra- and hexasaccharide fragments contain one and two intact units of the heparin disaccharides, respectively, in their interior. Microtitration calorimetry (16) provided dissociation constants for binding of bFGF to the tetrasaccharide and hexasaccharide of 6 ± 2 μM and 101 ± 1 nM, respectively, in 10 mM sodium phosphate and 1 mM dithiothreitol, pH 7.4. These fragments compete for FGF binding with heparin (10). Although heparin fragments with at least 12 to 14 residues are required for optimal FGF activity [A. Walker, J. E. Turnbull, J. T. Gallagher, *J. Biol. Chem.* **269**, 931 (1994)], FGF-mediated mitogenic activity of heparin hexasaccharide fragments has been demonstrated [T. Barzu, J. C. Lormeau, M. Petitou, S. Michelson, J. Choay, *J. Cell. Physiol.* **140**, 538 (1989); A. G. Gambarini, C. A. Miyamoto, G. A. Lima, H. B. Nader, C. P. Dietrich, *Mol. Cell. Biochem.* **124**, 121 (1993)].
10. H. Mach *et al.*, *Biochemistry* **32**, 5480 (1993).
11. Cocrystals of bFGF-heparin tetrasaccharide (space group $P2_12_12_1$ with a = 32.0 Å, b = 41.8 Å, and c = 85.9 Å) were grown with the vapor diffusion method, with 1.0 μl of heparin tetrasaccharide solution (20 mg/ml) added to 2.5 μl of bFGF solution (10 mg/ml) and 2.5 μl of reservoir solution [25% polyethylene glycol (PEG) (8 kD) and 0.1 M *N*-[2-acetamido]-2-iminodiacetic acid (ADA), pH 7.0]. These conditions correspond to about a 10:1 molar ratio of tetrasaccharide to bFGF. We used recombinant human bFGF with cysteines at residues 70 and 88 replaced by serines [G. M. Fox *et al.*, *J. Biol. Chem.* **263**, 18452 (1988)]. Cocrystals of bFGF-heparin hexasaccharide (space group $P2_12_12_1$ with cell dimensions of a = 33.1 Å, b = 41.9 Å, and c = 86.1 Å) were grown with the vapor diffusion method, with the use of 2.0 μl of heparin hexasaccharide solution (10 mg/ml) added to 2.5 μl of bFGF solution (10 mg/ml) and 2.5 μl of reservoir solution [34% PEG (8 kD), 30 mM $MgCl_2$, and 0.1 M ADA, pH 7.0]. This corresponds to about a 6:1 molar ratio of hexasaccharide to bFGF.
12. Tetrasaccharide-bFGF complex diffraction data were collected at room temperature with a Rigaku RAXIS-IIc imaging plate, integrated with Molecular Structure Corporation programs, and scaled and merged with CCP4 programs [S. Bailey, *Acta Crystallogr.* **D50**, 760 (1994)]. The final data set contained 9084 unique reflections to 1.9 Å resolution (95.6% complete), reduced from a total of 23,651 observations with a merging R factor of 0.071. Hexasaccharide-bFGF complex diffraction data were collected at room temperature with a Siemens area detector and processed with the program XDS [W. Kabsch, *J. Appl. Crystallogr.* **21**, 916 (1988)]. The final data set contained 6123 unique reflections to 2.2 Å resolution (94.7% complete), reduced from a total of 19,016 observations with a merging R factor of 0.073. This orthorhombic crystal form was previously observed for unliganded bFGF crystals crystallized from ammonium sulfate (17). This model was used to start iterative cycles of refinement with X-PLOR [A. T. Brünger, J. Kuriyan, M. Karplus, *Science* **235**, 458 (1987)] and model building with TOM-FRODO [T. A. Jones, *Methods Enzymol.* **115**, 157 (1985)] to complete the structures of both complexes. The bFGF-heparin tetrasaccharide structure was refined to R = 0.21 for data between 5.0 and 1.9 Å resolution, with $F > \sigma(F)$, and root-mean-square deviations for bond distances and angles from ideal values of 0.014 Å and 2.4°, respectively. The bFGF-heparin hexasaccharide structure refined to R = 0.19 for data between 6.0 to 2.2 Å resolution, with $F > \sigma(F)$, and root-mean-square deviations for bond distances and angles from ideal values of 0.015 Å and 2.4°, respectively. A total of 1068 atoms are presently in the bFGF-tetrasaccharide model (989 protein atoms, 70 heparin atoms, and 9 water atoms), whereas 1112 atoms are in the bFGF-hexasaccharide structure (993 protein atoms, 105 heparin atoms, and 14 water atoms). Residues 1 to 21 and the side chain of Arg^{61} are disordered in both structures, as well as the side chain of Glu^{79} in the tetrasaccharide, and hence are not included in the refined models. The terminal sugar unit at the nonreducing end of the tetrasaccharide has weaker electron density, indicating a somewhat disordered crystal. Coordinates have been deposited with the Brookhaven Protein Data Bank (entries 1BFB and 1BFC for the tetra- and hexasaccharide complexes of bFGF, respectively).
13. Superposition of the backbone Cα of different structures was performed with a program based on the algorithm of Kabsch [W. Kabsch, *Acta Crystallogr.* **A32**, 922 (1976)]. Helical parameters were determined as described [J. M. Cox, *J. Mol. Biol.* **28**, 151 (1967)] from the rotation and translation parameters obtained for the superposition of the ring atoms of GlcN-2 to Idu-3 onto GlcN-4 to Idu-5 in the middle of the hexasaccharide.
14. B. Mulloy, M. J. Forster, C. Jones, D. B. Davies, *Biochem. J.* **293**, 849 (1993).
15. J. J. Stoddart, *Stereochemistry of Carbohydrates* (Wiley-Interscience, New York, 1971).
16. L. D. Thompson, M. W. Pantoliano, B. A. Springer, *Biochemistry* **33**, 3831 (1994).
17. J. Zhang, L. S. Cousens, P. J. Barr, S. R. Sprang, *Proc. Natl. Acad. Sci. U.S.A.* **88**, 3446 (1991).
18. A. Baird, D. Schubert, N. Ling, R. Guillemin, *ibid.* **85**, 2324 (1988); J. W. Harper and R. R. Lobb, *Biochem-*

istry **27**, 671 (1988); R. R. Lobb, *ibid.*, p. 2572.
19. X. Zhu *et al.*, *Science* **251**, 90 (1991).
20. A. E. Eriksson, L. S. Cousens, L. H. Weaver, B. W. Matthews, *Proc. Natl. Acad. Sci. U.S.A.* **88**, 3441-3445 (1991); H. Ago, Y. Kitagawa, A. Fujishima, Y. Matsura, Y. Katsube, *J. Biochem.* **110**, 360 (1991); E. Eriksson, L. S. Cousens, B. W. Matthews, *Protein Sci.* **2**, 1274 (1993).
21. X. Zhu, B. T. Hsu, D. C. Rees, *Structure* **1**, 27 (1993).
22. D. M. Ornitz *et al.*, *Science* **268**, 432 (1995).
23. B. Lee and F. M. Richards, *J. Mol. Biol.* **55**, 379 (1971).
24. M. Miyamoto *et al.*, *Mol Cell. Biol.* **13**, 4251 (1993).
25. R. Reichslotky *et al.*, *J. Biol. Chem.* **269**, 32279 (1994).
26. D. J. Austin, G. R. Crabtree, S. L. Schreiber, *Chem. Biol.* **1**, 131 (1994).
27. T. Arakawa, J. Wen, J. S. Philo, *Arch. Biochem. Biophys.* **308**, 267 (1994).
28. P. J. Kraulis, *J. Appl. Crystallogr.* **24**, 946 (1991).
29. Abbreviations for the amino acid residues are as follows: A, Ala; C, Cys; D, Asp; E, Glu; F, Phe; G, Gly; H, His; I, Ile; K, Lys; L, Leu; M, Met; N, Asn; P, Pro; Q, Gln; R, Arg; S, Ser; T, Thr; V, Val; W, Trp; and Y, Tyr.
30. Wisconsin Sequence Analysis Package, version 8, Genetics Computer Group, Madison, WI.
31. We thank T. Arakawa and G. M. Fox of Amgen for discussions and a generous supply of bFGF and D. Bar-Shalom for stimulating conversations. This work was funded in part by a gift from Amgen and U.S. Public Health Service (USPHS) grant GM38060 (R.J.L.), with partial support of the x-ray facility provided by the Beckman Institute at California Institute of Technology and USPHS grant GM45162 (D.C.R.). S.F. was supported by USPHS Biotechnology Training grant T32 GM08346.

19 September 1995; accepted 12 December 1995

The p21^{RAS} Farnesyltransferase α Subunit in TGF-β and Activin Signaling

Tongwen Wang,* Paul D. Danielson, Bi-yu Li, Paresh C. Shah, Stephen D. Kim, Patricia K. Donahoe*

The α subunit of p21^{RAS} farnesyltransferase (FNTA), which is also shared by geranylgeranyltransferase, was isolated as a specific cytoplasmic interactor of the transforming growth factor–β (TGF-β) and activin type I receptors with the use of the yeast two-hybrid system. FNTA interacts specifically with ligand-free TGF-β type I receptor but is phosphorylated and released upon ligand binding. Furthermore, the release is dependent on the kinase activity of the TGF-β type II receptor. Thus, the growth inhibitory and differentiative pathways activated by TGF-β and activin involve novel mechanisms of serine-threonine receptor phosphorylation–dependent release of cytoplasmic interactors and regulation of the activation of small G proteins, such as p21^{RAS}.

Cell growth and differentiation are regulated and delicately balanced by the activities of growth stimulators and suppressors. Although much is known about growth stimulatory pathways that act by means of tyrosine kinase receptors (*1*), little is known about the growth inhibitory pathways exemplified by the serine-threonine kinase receptors of the TGF-β family. Recent progress in cloning and characterization of the TGF-β family receptors revealed that two membrane serine-threonine kinases, the type I and type II receptors, form heteromeric complexes. In this functional signaling unit, the TGF-β type II receptor phosphorylates and possibly thereby activates the type I receptor to signal downstream pathways (*2*, *3*). However, the molecular mechanisms involved in the activation of type I receptor–mediated signaling will remain unknown until direct downstream cytoplasmic interactors are identified.

Because conventional biochemical methods to isolate cytoplasmic proteins in tyrosine kinase receptor downstream pathways have not identified intracellular interactors of the serine-threonine kinase receptors, we used a modified version of the yeast two-hybrid system (*4*, *5*). As determined by binding and functional assays (*6*, *7*), the cytoplasmic domain of the TGF-β type I receptor, also known as ALK5 (*6*) and R4 (*8*), was used as a bait to screen a human fetal brain library (Fig. 1A). Three groups of interactors were identified: human immunophilin FKBP12 (*9*) and two versions of the human FNTA (*10*) (Fig. 1B). The latter differ within the 10 COOH-terminal amino acids, the region least conserved among species (*10*) and critical for farnesyltransferase enzyme activity (*11*). Regulation of the expression of these two variants may be important in controlling the activities of the enzyme in vivo.

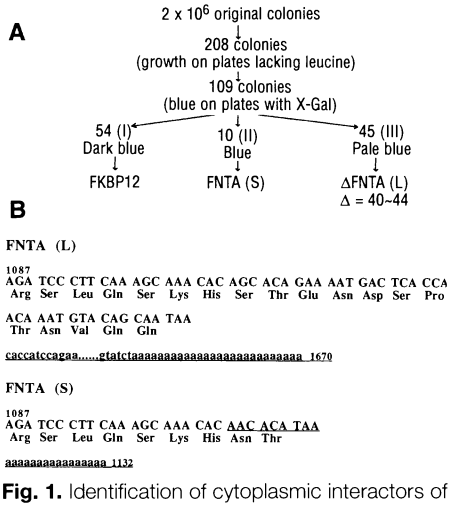

Fig. 1. Identification of cytoplasmic interactors of the TGF-β type I receptor (R4) with the use of a modified yeast two-hybrid system (*4*, *5*). (**A**) Summary of the library screening. The entire cytoplasmic domain of R4 was fused in-frame to the COOH-terminus of the DNA binding domain of LexA to serve as the bait (*5*). A human fetal brain complementary DNA (cDNA) library in the yeast expression vector pJG4-5 was used in the library screening. (**B**) Difference of the nucleotide sequences and their encoded amino acid sequences of the two isolated FNTA cDNAs. L, long; S, short.

When tested in the yeast system (Fig. 2A), the α subunit interacted with the β subunit of farnesyltransferase (FNTB) as expected and also interacted specifically with the functional type I receptors of TGF-β (R4) and activin (R2) among all tested type I receptors (*6*–*8*, *15*). The R4-FNTA interaction appeared not to be dependent on the kinase activity of R4 and was specific for type I receptors, because a kinase-deficient R4 [Fig. 2A, R4(K230R)] (*16*) was still capable of FNTA binding. Neither of the type II receptors of TGF-β and activin exhibited FNTA binding (*17*). The NH_2-terminal 81 amino acids of the α subunit, important for the enzyme activity of FTase in mammalian cells (*11*), were also essential for R4 binding [Fig. 2A, R4(Δ81)FNTA].

The cytoplasmic region of R4 (R4C) contains the juxtamembrane (JM), the serine-threonine kinase (K), and the tail

Pediatric Surgical Research Laboratories, Massachusetts General Hospital, Boston, MA 02114, USA.

*To whom correspondence should be addressed. E-mail: Donahoe@helix.mgh.harvard.edu